Supplementary Information

Two-photon Fluorogenic Probe Visualizing PGP-1 Activity in Inflammatory Tissue and Serum from Patients

Hua Bai,‡[ae] *Bin Fang,*‡[ac] *Xujie Wang,*‡[b] *Wenjing Qin,*[d] *Yuhe Chen,*[a] *Dongliang Zhang,*[b] *Yan Li,*[b] Bo Peng,[ae] *XuekangYang,**[b] *Li Fu**[c] *and Lin Li**[a]

[a] *Frontiers Science Center for Flexible Electronics, Xi'an Institute of Flexible Electronics (IFE) and Xi'an Institute of Biomedical Materials & Engineering, Northwestern Polytechnical University, 127 West Youyi Road, Xi'an 710072, P. R. China. E-mail: iamlli@nwpu.edu.cn*

[b] *Department of Burns and Cutaneous Surgery, Xijing Hospital, The Fourth Military Medical University, Xi'an, 710032, P. R. China. E-mail: yangxuekangburns@163.com*

[c] *State Key Laboratory of Solidification Processing, School of Materials Science and Engineering, Northwestern Polytechnical University, 127 West Youyi Road, Xi'an 710072, P. R. China. E-mail: fuli@nwpu.edu.cn*

[d] *Key Laboratory of Flexible Electronics (KLOFE) & Institute of Advanced Materials (IAM), Nanjing Tech University (NanjingTech) 30 South Puzhu Road, Nanjing, 211816, P. R. China*

[e] *Ningbo Institute of Northwestern Polytechnical University, Ningbo 315103, China.*

‡*These authors contributed equally to this work*

Table of Contents

1. Supplementary methods

All chemicals were purchased from Aldrich or TCI unless otherwise indicated, and used without further purification. All non-aqueous reactions were carried out under a nitrogen/argon atmosphere in oven-dried glasswares. Anhydrous solvents for organic synthesis were distilled over CaH_2. Reaction progress was monitored by TLC on pre-coated silica plates (250 μm thickness) and spots were visualized by UV light or iodine. Flash column chromatography was carried out using silica gel (Merck 60 $F_{254\ nm}$ 0.040-0.063 μm). ^1H and ^{13}C NMR spectra were measured with an AVANCE NEO 500 by using $CDCl_3$ and DMSO-d_6 as solvents. Chemical shifts are reported in parts per million referenced with respect to residual solvent ($CDCl_3$ = 7.26 ppm, DMSO-d_6 = 2.50 ppm for ^1H NMR; $CDCl_3$ = 77.16 ppm, DMSO-d_6 = 39.52 ppm for ^{13}C NMR). Coupling constants (*J* value) are reported in Hz. Pyroglutamate Aminopeptidase 1 (PGP-1, M7316 and M7441, 2 U/mg) were purchased from Shanghai Fudan-Zhangjiang Bio-Pharmaceutical Co., Ltd. PGP-1 inhibitor: iodoacetamide (I6125) and Lipopolysaccharides (LPS, L2630) were purchased from Sigma. Anti-PGP-1 (19566-1-AP) and anti-beta Actin (4967) antibodies were purchased from Proteintech and Cell signaling technology, respectively. Human TNF-α ELISA kit (EHC103a.96) and Human IL-6 ELISA kit (EHC007.96) were purchased from Neobioscience. Procalcitonin (PCT) diagnostic reagents were purchased from Roche and electrochemiluminescence were recorded using Cobas E601 module (Roche). Ultrapure water was used to prepare all aqueous solutions.

Analytical HPLC (DIONEX Ultimate 3000) and Mass spectra were recorded on a THERMO ISQ-EC LC-MS system equipped with a VWD3100 UV-vis detector, the detection wavelength for HPLC profiles is 254 nm, and an autosampler, using reverse-phase Hypersil GOLD^{TM} 250 × 4.6 mm columns. 0.1% Formic acid (FA)/H_2O and 0.1% FA/acetonitrile were used as eluents (flow rate was 1 mL/min). The UV-visible absorption spectra of dilute solutions were recorded using a U-3900H spectrophotometer using a quartz cuvette with a 1 cm path length. One-photon fluorescence spectra were obtained using a HITACHI F-7100 spectrofluorimeter equipped with a 450 W Xe lamp. Enzymatic assays were recorded by multi-mode microplated reader (Tecan spark) Histology imaging were obtained by Olympus FSX100 Bio Imaging Navigator. Cell fluorescent imaging were obtained by Nikon C2 confocal microscope system. Tissue fluorescent imaging were obtained by Zeiss LSM 880 system. Images were processed with Zeiss User PC Advanced for LSM system (BLUE). Cell flow cytometer were obtained by Beckman CytoFLEX S system. All measurements were performed at room temperature.

Preparation of phosphate buffer saline (PBS):

KH_2PO_4 (0.12 g), Na_2HPO_4•$12H_2O$ (1.79 g), NaCl (4.0 g) and KCl (0.1 g) was dissolved in ultrapure water (400 mL). Hydrochloric acid was added to adjust the pH

value to 7.4. Then ultrapure water was added to the solution up to 500 mL and it was placed at 120 °C and 0.1 Mpa for 20 minutes before use.

Preparation of various ROS and RNS species:

$ONOO^-$: To a vigorously stirred solution of $NaNO_2$ (0.6 M, 10 mL) and H_2O_2 (0.7 M, 10 mL) in deionized H_2O at 0 °C was added HCl (0.6 M, 10 mL), immediately followed by the rapid addition of NaOH (1.5 M, 20 mL). Excess hydrogen peroxide was removed by passing the solution through a short column of MnO_2. The concentration of $ONOO^-$ was determined by UV analysis with the extinction coefficient at 302 nm (ε= 1670 M^{-1} cm^{-1}). Aliquots of the solution were stored at -20 °C for use.

NO: A solution of the H_2SO_4 (3.6 M) was added dropwise into a stirred solution of $NaNO_2$ (7.3 M). The emitted gas was allowed to pass through a solution of NaOH (2 M) first and then deionized H_2O to make a saturated NO solution of 2.0 mM.

$^1O_2$: $NaMoO_4$ (10 mM) and H_2O_2 (10 mM) was prepared in PBS (10 mM, pH 7.4). Equal aliquots of these solutions were then mixed to yield $^1O_2$ of 5 mM.

H_2O_2 and NaClO: H_2O_2 and NaClO solution were prepared by diluting commercial H_2O_2 and NaClO solutions with PBS (10 mM, pH 7.4) to make 10 mM stock solutions.

•OH: •OH was generated by Fenton reaction. To a solution of H_2O_2 (1.0 mM, 1.0 mL) in PBS (10 mM, pH 7.4) was added $FeSO_4$ solution (1.0 mM, 100 μL) at ambient temperature (stock solution 0.1 mM).

ROO•: ROO• was generated from 2, 2'-azobis(2-amidinopropane)dihydrochloride, which was dissolved in PBS (10 mM, pH 7.4) 1 h before use to make a stock solution of 10 mM.

2. Chemical Synthesis

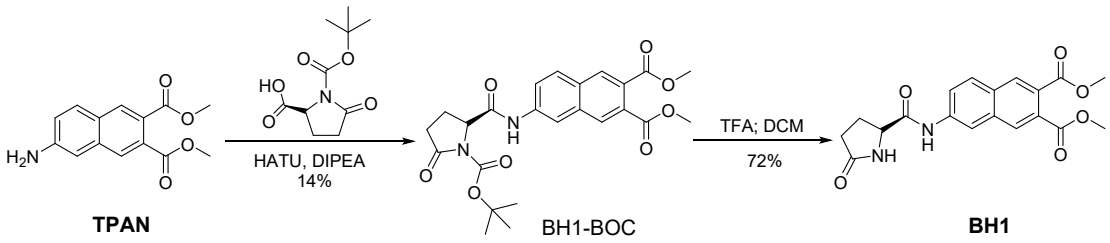

Scheme S1 The synthetic route of two-photon small molecular fluorogenic probe (**BH1**).

Synthesis of TPAN. TPAN was synthesized according to the previous report methods.[1] ^1H NMR (500 MHz, DMSO-d_6) δppm: 8.22-8.12 (m, 1H), 7.84-7.70 (m, 2H), 7.08 (dd, J = 8.7, 2.2 Hz, 1H), 6.91 (s, 1H), 5.96 (s, 2H), 3.81 (t, J = 3.1 Hz, 6H).

Synthesis of BH1-BOC. (S)-Boc-5-oxopyrrolidine-2-carboxylic acid (115 mg, 0.5 mmol), HATU (190 mg, 0.5 mmol), and DIPEA (200 μL, 1.25 mmol) were dissolved in dry dichloromethane (DCM, 5 mL) with stirring at 0 °C for 30 min. Then, **TPAN** (130 mg, 0.5 mmol) in DCM (5 mL) was introduced, and the reaction mixture was further stirred at room temperature for 4 h. The precipitate was filtered, and the filtrate was evaporated under reduced pressure. The residue was purified by silica gel chromatography with petroleum ether/ethyl acetate (30/1 to 1/1, v/v) as eluent, yielding BH1-BOC as an dark red solid (70 mg; yield 14%). ^{1}H NMR (500 MHz, DMSO-d_6) δppm: 10.80 (s, 1H), 8.44 (s, 1H), 8.36 (s, 1H), 8.24 (s, 1H), 8.13 (d, J = 8.7 Hz, 1H), 7.85 (d, J = 8.4 Hz, 1H), 4.75 (d, J = 6.3 Hz, 1H), 3.86 (s, 6H), 2.38-2.17 (m, 2H), 2.40-2.26 (m, 2H), 1.98 (s, 2H), 1.36 (s, 9H). ^{13}C NMR (125 MHz, DMSO-d_6) δppm: 177.49, 172.04, 167.79, 167.13, 139.19, 133.80, 129.89, 129.72, 129.37, 129.23, 128.78, 126.05, 122.51, 115.77, 56.49, 52.60, 29.22, 25.33. HRMS: *m/z* $[M+H]^+$ calcd: 471.5263, found: 470.1689.

Synthesis of BH1. BH1-BOC (70 mg, 0.15 mmol) was dissolved in dry DCM (5 mL). Trifluoroacetic acid (2 mL) in DCM (3 mL) was added dropwise to the solution of the above intermediate, and the reaction mixture was stirred at room temperature for 3 h. The solvent was removed by evaporation under reduced pressure, and the crude product was purified by flash silica gel chromatography eluted with DCM/methanol (10/1, v/v), affording **BH1** as a crimson solid (50 mg, yield 72%). ^{1}H NMR (500 MHz, $CDCl_3$) δppm: 8.96 (s, 1H), 8.17 (s, 1H), 8.05 (s, 1H), 7.99 (s, 1H), 7.69 (d, J = 8.7 Hz, 1H), 7.62 (d, J = 8.6 Hz, 1H), 7.09 (s, 1H), 4.39 (dd, J = 8.3, 5.5 Hz, 1H), 3.94 (s, 3H), 3.91 (s, 3H), 2.66 (s, 1H), 2.52 (s, 1H), 2.43 (s, 1H), 2.34 (s, 1H). ^{13}C NMR (125 MHz, $CDCl_3$) δppm: 177.49, 172.04, 167.79, 167.13, 139.19, 133.80, 129.89, 129.72, 129.37, 129.23, 128.78, 126.05, 122.51, 115.77, 56.49, 52.60, 29.22, 25.33. HRMS: *m/z* $[M+H]^+$ calcd: 370.3610, found: 371.2272.

3. Experimental procedures

3.1. Molecular docking

In order to demonstrate the specific recognition of **BH1** by PGP-1, molecular docking experiments were carried out by using Autodock Vina software (version 1.56, The Scripps Research Institute). Explicit hydrogen atoms were added, all water molecules were then deleted. The ligand was removed, and the protein structure was processed by using AutoDock Tools. **BH1** was prepared for docking by using AutoDock Tools to assign AD4 atom types, calculate Gasteiger charges, and set all rotatable bonds as active torsions. PGP-1 protein model with PDB identification code of LIU8 was selected, and the docking region was selected near the main catalytic sites GLU-76, CYS-13 and HIS-163 at the meantime, the binding energy is calculated. Autodock Vina software was used as a viewer for interaction between ligands and protein receptor.

3.2. The fluorescence quantum yields

Fluorescence quantum yield (Φ) of compounds were determined to that of Coumarin 307 (Φ = 0.56 in EtOH) by using the following equation: $\Phi_s = \Phi_r (A_r n_s^2 D_s / A_s n_r^2 D_r)$, where the s and r indices designate the sample and reference samples, respectively, A is the absorbance at λ_{ex}, n is the average refractive index of the appropriate solution, and D is the integrated area under the corrected emission spectrum.

3.3. Cell culture and treatment

Human acute monocytic leukemia cell line (Thp1), human hepatocellular carcinoma (HepG2), human neuroblastoma (SH-SY5Y) and mouse macrophage cell line (RAW264.7) were obtained from the American Type Culture Collection (ATCC), and cultured in Dulbecco's Modified Eagle Medium (DMEM; Hyclone) or RPMI 1640 Medium (Hyclone), supplemented with 10% fetal bovine serum (FBS; Biological Industries) and 100 μg/mL penicillin/streptomycin. The cells were incubated at 37°C in a humidified atmosphere of 5% CO_2. For LPS stimulation, 24 h after cells were plated in 35-mm dishes at a density of 1×10^5/mL, the culture medium was replaced with fresh complete medium and cells were treated with LPS (1 μg/mL) for 8 h. For siRNA transfection, RAW264.7 cells were cultured for 24 h reaching ~70% confluence, and received non-targeting scramble, PGP-1 specific siRNA duplexes (5'-GATGCTGGCAGGTATCTGT-3'; TSINGKE Biological Technology) at the working concentration of 300 nM in each transfection system. Lipofectamine RNAiMAX (Invitrogen) was used as the transfection reagent. The transfection reaction was terminated 24 h later by replacing the medium containing siRNA and Lipofectamine RNAiMAX with fresh complete medium.

3.4. Quantitative real-time PCR (RT-qPCR)

Total RNA was extracted by using TRIzol reagent (Invitrogen) after the indicated treatments. In total, 500 ng of isolated RNA was reverse transcribed into complementary DNA using a PrimeScript RT Reagent Kit (Takara). RT-qPCR was performed with a CFX Connected real-time system (Bio-Rad) using UltraSYBR Green Mixture (Takara) and specific primers (Table S1). The amplification conditions were initial denaturation at 95°C for 30 s, followed by 40 cycles of 95°C for 5 s and 60°C for 30 s. Each sample was run in triplicate. The specificity of PCR products was confirmed by melting curve analysis. Relative expression was quantified by the $2^{-\Delta\Delta Ct}$ method. GAPDH was used as the housekeeping gene to normalize gene expression levels.

3.5. Western blot analysis

Normal and inflammatory skin tissues were from three patients during their wound tissue excision surgery in Department of Burns and Cutaneous Surgery, Xijing hospital. After being washed three times with ice-cold PBS, approximately 20 mg samples from dermis were collected in RIPA lysis buffer supplemented with protease and phosphatase inhibitor mixtures. Samples then received ultrasonic decomposition on ice followed by centrifugation at 12,000 × *g* at 4°C for 15 min to obtain supernatants. Lysates from cell

cultures were directly obtained using RIPA buffer freshly replenished with protease and phosphatase inhibitors, followed by lysed on ice for 15 min and then centrifuged at 12,000 × *g* at 4℃ for 15 min to collect soluble fractions. Protein concentration was determined by BCA assay with a Tecan microplate reader.

Next, 20 μg/sample of protein was separated via 10% SDS-PAGE and transferred onto PVDF membranes. The membranes were blocked with 5% skim milk for 1 h at room temperature, and then incubated with primary antibodies targeting PGP-1 (1 : 1000 dilution), or β-actin (1 : 10000 dilution) overnight at 4℃. The following day, membranes were washed three times with T-TBS buffer for 10 min each, and applied with HRP-conjugated secondary antibodies. Immunoreactive signals were detected by the enhanced chemiluminescent reaction. Images were acquired using a Bio-Rad ChemiDoc Imaging System. The intensity of each band was quantified using ImageJ software (NIH).

3.6. Cell imaging and flow cytometer experiment

Before cell imaging, the culture media were removed, cells were washed with PBS (3×). Then, the cells were incubated with **BH1** (5 μM) at 37°C for 2 h in culture medium, washed with PBS to remove the free probe, and finally were preserved in phenol free culture medium for fluorescent imaging (Nikon C2 confocal microscope system, $\lambda_{ex/em}$ = 405/535 nm) or flow cytometer (Beckman CytoFLEX S system, $\lambda_{ex/em}$ = 405/535 nm) experiments.

3.7. Cell viability assay

Cell viability was analyzed using PrestoBlue™ cell viability reagent (Invitrogen, Carlsbad, CA). Briefly, PrestoBlue™ was diluted 10 × with fresh medium and, then, supplied directly to cells. After incubation at 37°C for 1 h, the absorbance was read at 570 nm using a microplate reader (Infinite M200 Pro, Tecan, Switzerland). The cell data are expressed as a percentage of untreated control cells. Higher absorbance values correlate to greater total metabolic activity.

3.8. Human serum and skin tissue samples

The serum samples for detection of PGP-1, IL-6, TNF-α and PCT were from burn patients conformed to clinically diagnostic criteria of sepsis (n = 7, 3 female and 4 male, aged between 27-56 years old) and patients with scar hospitalized for plastic surgery (n = 7, 4 female and 3 male, aged between 24-60 years old). Inflammatory skin tissues and self-control normal skin tissues were collected from three patients (2 female and 1 male, aged 20, 35 and 50 years old) who were admitted to hospital for inflammatory wound excision and repairation. All patients were from department of burns and cutaneous surgery, Xijing hospital, the fourth military medical university. The study protocol was approved by the hospital ethics committee.

3.9. Hematoxylin and eosin (H&E) staining

The dermis samples were fixed with 4% paraformaldehyde, dehydrated in graded ethanol, embedded in paraffin, and then cut into 5 μm thick sections. H&E staining was used to detect the histological changes. Images were obtained by FSX100 Bio Imaging Navigator (Olympus).

3.10. Human skin tissues imaging

The human skin tissue specimens mentioned above were cut into slices of 150 μm as fast as possible by freezing microtome (Leica CM1950, Germany). Slices were incubated with **BH1** (5 μM) for 2 h, then imaged after washing by PBS (3×). To detect PGP-1 activity, slices were imaged by TPFM (Zeiss LSM 880, Germany) at the corresponding excitation wavelengths (λ_{ex} = 760 nm).

3.11. ELISA assay

The dermis tissue was homogenized and centrifuged at 15,000 × *g* at 4℃ for 20 min to obtain total proteins. TNF-α level of dermis tissue was quantified by ELISA assay kit according to the manufacturer's instructions (EHC103a.96, Neobioscience). Human blood samples were collected and centrifuged at 3000 rpm for 10 min. The upper layer of serum was assayed using ELISA assay kits to detect the levels of IL-6 and TNF-α.

3.12. Detection of PGP-1 activity in Human serum

These serum samples were taken from different patients in Xijing Hospital as described above, and frozen immediately after sampling. Before use, the blood samples were centrifuged (3000 rpm, 5 min), and the clarified supernatant obtained was the serum. The serum was extracted with a syringe and filtered with a 0.45 μm microporous filter. The fluorescence intensity of serum samples was measured by fluorescence spectrophotometer (λ_{ex} = 350 nm, Hitachi F-7000 fluorescence spectrophotometer); after incubating the serum samples with **BH1** for 2 h, the fluorescence intensity was tested again. The results of deducting the background fluorescence intensity of serum were used to detect the contents of PGP-1 in serum samples.

4. Supplementary figures

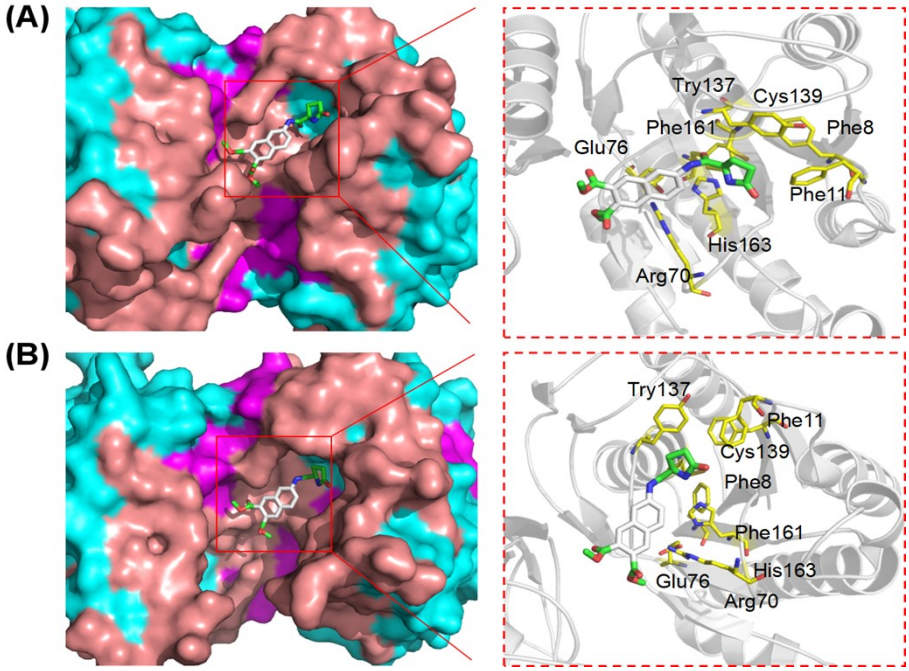

Fig. S1 (A) The binding mode of **BH1** with PGP-1 (PDB: LIU8). (B) Schematic drawing around the active site of PGP-1. The figure was produced with Autodock Vina software. Glu-76, Cys-139, and His-163 are three main catalytic sites. The catalytic domain consists of the main protein residues: Arg-70, His-163, Glu-76, Phe-161, Cys-139, Tyr-137, Phe-8, and Phe-11.

The stock solution of probe **BH1** (10 mM) was prepared in Dimethyl sulfoxide (DMSO) and stored at 4 oC. All spectroscopic study of probe was carried out in test solution of probe (5 μM) in 2 mL PBS (10 mM PBS, pH = 7.42, containing 0.5 % DMSO), which was prepared by adding 10 μL probe stock solution into buffer in a quartz cuvette. After measuring the emission and absorption spectra of the test solution.

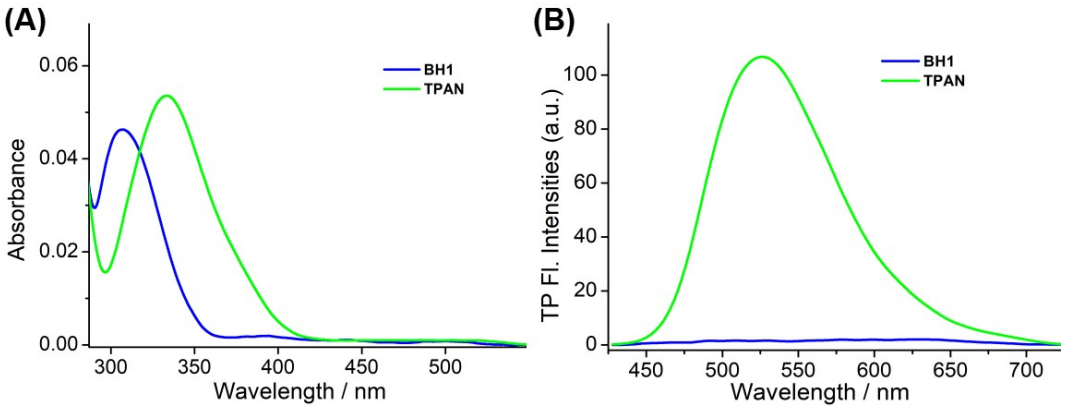

Fig. S2 (A) Absorption spectra of **BH1** (5 μM) and **TPAN** (5 μM) in phosphate buffer

saline (10 mM PBS; pH 7.42; containing 0.5 % DMSO). (B) The two-photon excited fluorescence (TPEF) spectra of **BH1** and **TPAN** excited by the input laser power at the optimum wavelength (760 nm) in PBS buffer solution.

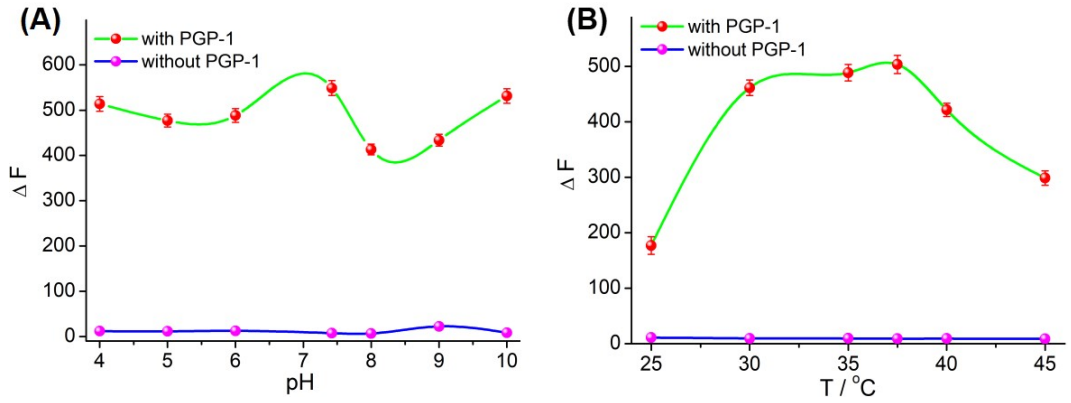

Fig. S3 Effects of reaction temperature and pH on the fluorescence of **BH1** (5 μM) with (green line) and without (blue line) PGP-1 (0.5 μg/mL). Conditions: (A) the reaction was performed in PBS (10 mM; pH 7.42; containing 0.5 % DMSO) for 2 h at different pH values adjusted with dilute HCl or NaOH; (B) the reaction was performed in PBS for 2 h at different temperature; $\lambda_{ex/em}$ = 335/515 nm.

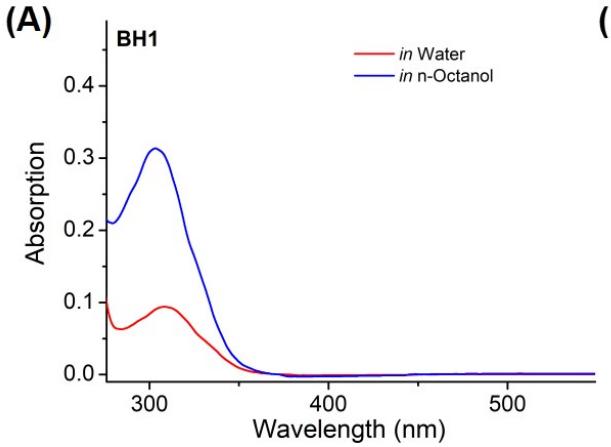

(B)

Solvent	Absorbance	$P_{oct/wat}$	$logP_{oct/wat}$
Water	0.094	3.298	0.518
n-Octanol	0.310		

Fig. S4 (A) Absorption spectra of **BH1** (5 μM) in water and n-Octanol (containing 0.5 % DMSO). (B) Relevant data of the oil-water partition coefficient log $P_{oct/wat}$.

There are many factors affecting the membrane permeability of substances, among which the main factors are molecular weight, lipophilicity and electrification. The probe **BH1** is a relative molecular mass (371.22) of <500, and its oil-water partition coefficient log Poct/wat (lipophilicity) of 0.52, which is related to solubility and permeability, meets the range of log P < 5.[3] In addition, **BH1** is a lipophilic neutral molecule, so it is easy to penetrate the cell membrane. [4]

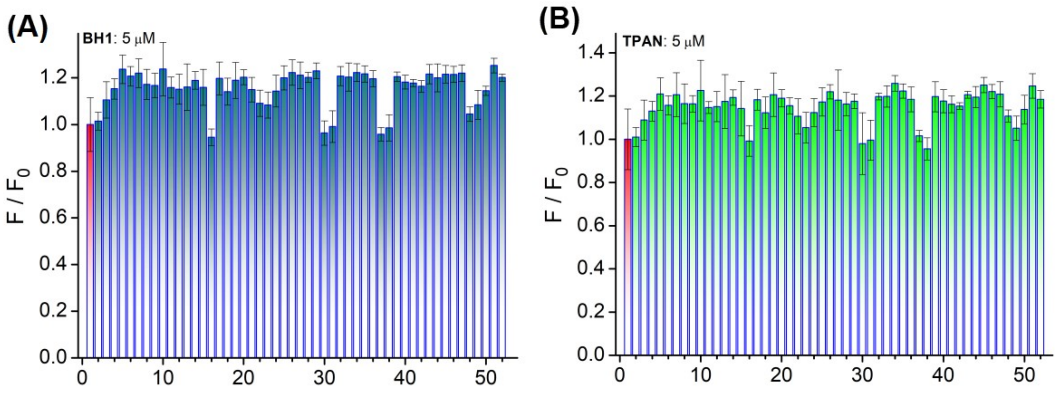

Fig. S5 Fluorescence response of **BH1** (5 μM) and **TPAN** (5 μM) to various analytes (10eq.) after 2 h incubation in PBS buffer (pH 7.42). 1. **BH1**/**TPAN**; 2. NaCl; 3. KNO_3; 4. $Mg(NO_3)_2$•$6H_2O$; 5. $Al(NO_3)_3$•$9H_2O$; 6. $Cu(NO_3)_2$•$9H_2O$; 7. $Fe(NO_3)_3$•$9H_2O$; 8. $Mn(NO_3)_2$•$4H_2O$; 9. $Cd(NO_3)_2$•$4H_2O$; 10. $Zn(NO_3)_2$•$6H_2O$; 11. $Ni(NO_3)_2$•$6H_2O$; 12. $Cr(NO_3)_3$•9H2O; 13. $FeCl_2$•$4H_2O$; 14. $Ca(NO_3)_2$•$4H_2O$; 15. CH_3COONa; 16. $NaHCO_3$; 17. NaF; 18. NaBr; 19. NaI; 20. $NaNO_3$; 21. Na_2CO_3; 22. Na_2SO_4; 23. Na_2HPO_4•$12H_2O$; 24. NaH_2PO_4•$2H_2O$; 25. NaClO; 26. Glycine; 27. Alanine; 28. Valine; 29. Isoleucine; 30. Phenylalanine; 31. Tryptophan; 32. Methionine; 33. Proline; 34. Serine; 35. Threonine; 36. Cysteine; 37. Tyrosine; 38. Histidine; 39. Lysine; 40. Arginine; 41. Aspartic acid; 42. Glutamic acid; 43. GSH; 44. HS^-; 45. S^{2-}; 46. H_2O_2; 47.•OH; 48. ONOO-; 49. NO; 50. $^1O_2$; 51. ROO•; 52. Total protein of HepG 2. Data are presented as the mean ± SD (n = 3).

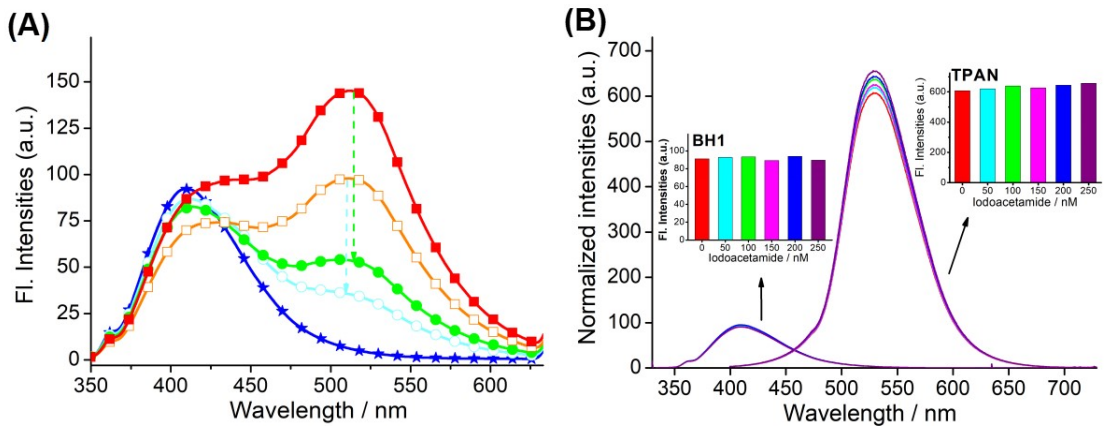

Fig. S6 (A) Fluorescence emission spectra of different reaction systems. (—★—solid pentagonal blue curve) **BH1** only (5 μM); (—□—hollow square orange curve) **BH1** (5 μM) + PGP-1 (300 ng/mL); (—○—hollow circular cyan curve) **BH1** (5 μM) + PGP-1 (300 ng/mL) + iodoacetamide (150 nM); (—■—solid square red curve) **BH1** (5 μM) + PGP-1 (500 ng/mL); (—●—solid circular green curve) **BH1** (5 μM) + PGP-1 (500 ng/mL) + iodoacetamide (250 nM). Addition of the inhibitor (iodoacetamide) largely decreases the fluorescence of the reaction system *via* inhibiting the PGP-1 activity. (B) Effects of iodoacetamide on the fluorescent intensity of the **BH1** and **TPAN**.

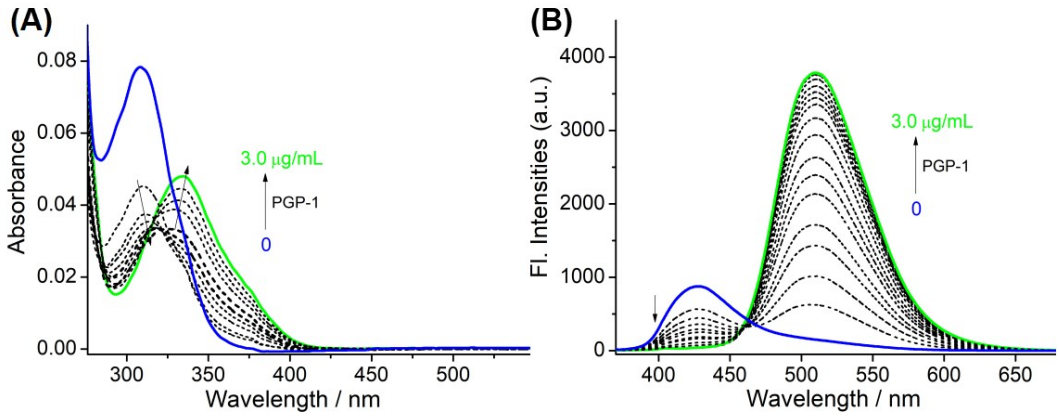

Fig. S7 The UV-vis spectra and fluorescence response of **BH1** (3 μM) to PGP-1 upon 5 days incubation with different concentrations (from bottom to top: 0-3.0 μg/mL).

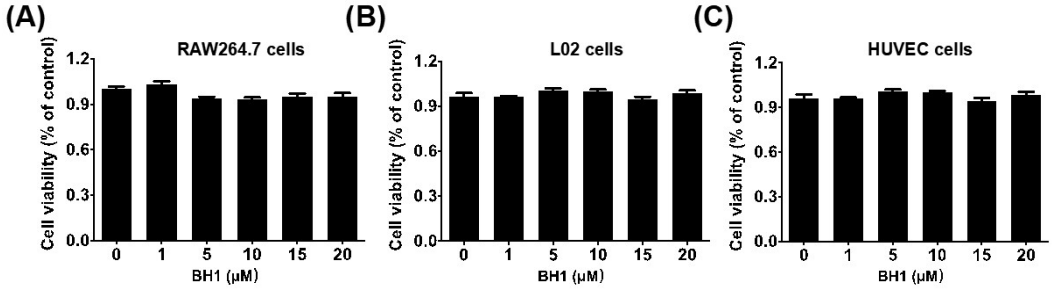

Fig. S8. Effects of probe (**BH1**) at varied concentrations on the viabilities of RAW264.7 cells (A), L02 cells (B), HUVEC cells (C).

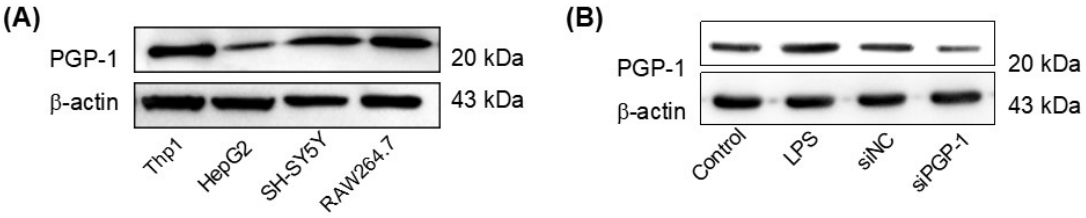

Fig. S9. (A) Corresponding protein and gene expression levels of PGP-1 in Thp1, HepG2, SH-SY5Y and RAW264.7 cells were detected by western blot (WB), β-actin was used as loading control. The WB values are shown as folds of Thp1. (B) Protein and gene expressions of PGP-1 in whole cell lysates were detected by WB in RAW264.7 cells. The WB values are shown as folds of control.

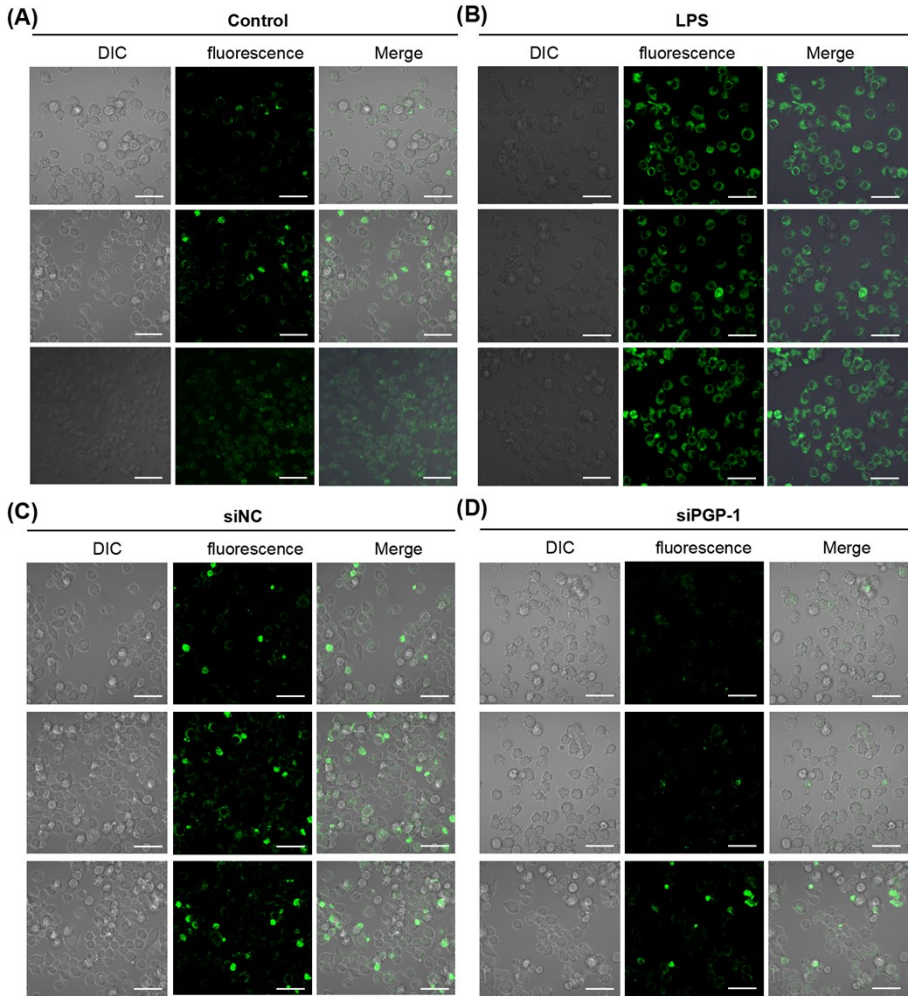

Fig. S10. Representative OPFM images of the living RAW264.7 cells upon incubation with **BH1** (5 μM, 1 h) after LPS or siRNA treatment. Scale bar = 50 μm.

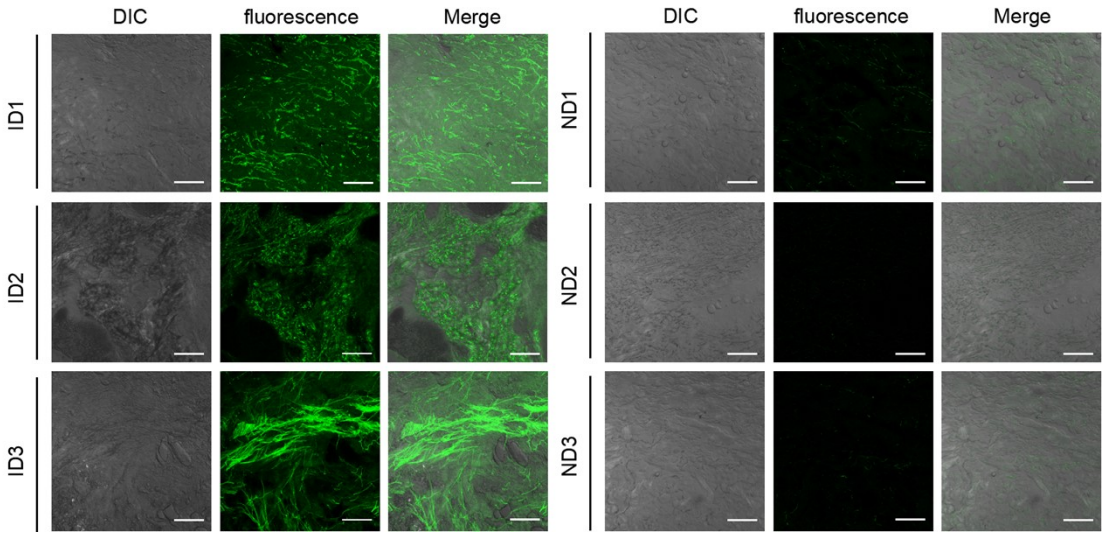

Fig. S11. TPFM images of the activity of endogenous PGP-1 with **BH1**-treated (5 μM, 2 h) fresh human inflammatory dermal (ID) and self-control normal dermal (ND). Scale

bar = 100 μm.

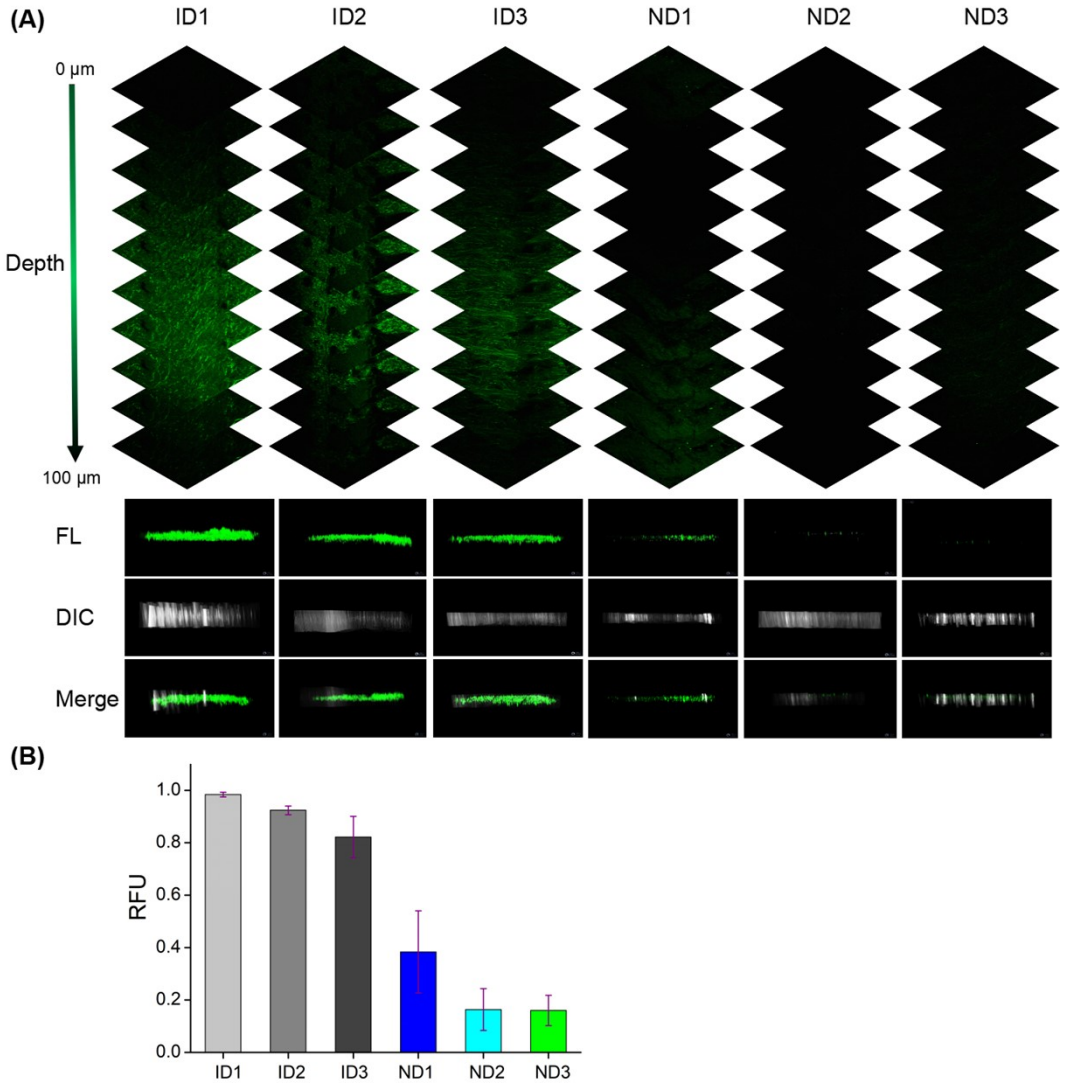

Fig. S12 (A) TPFM images of endogenous PGP-1 activity and the corresponding quantified fluorescence intensity (B) of **BH1**-treated (5 μM, 2 h) human inflammatory dermal (ID) and self-control normal dermal (ND). Error bars represent standard error of the mean. Data are presented as the mean ± SD (n = 3).

Table. S1 The basic photophysical properties and enzyme kinetic data of **BH1** and **TPAN**.

Comp.	λ[a]	Φ[b]	$\delta\Phi$/ GM[c]	K_{app} x 10^{-4} ($M^{-1}\cdot min^{-1}$)	K_m (μM)	K_{cat} (min^{-1})	V_{max} ($nmol\cdot mg^{-1}\cdot min^{-1}$)
TPAN	335/513	0.283	188.0	-/-	-/-	-/-	-/-
BH1	300/408	0.136	12.4	0.043	8.996	0.38	0.11

[a] the optimal peak positions of the absorption and emission spectra; [b] the fluorescence quantum yields (Φ) determined by using fluorescein as coumarin 307 (Φ = 0.85, in EtOH) standard; [c] the maxima two-photon action cross section values upon excitation wavelength of fluorophore from 700 to 980 nm in GM (1 GM = 10-50 cm4 s photon-1); -/-: not determined.

Table S2. Primers used for RT-qPCR in this study.

Gene	Primer sequence	Orientation	A.T. (℃)	GenBank Accession no.
PGP-1 (Human)	5'-CGACCACAGTCACACTGGAG-3'	sense	60	NM_017712.4
	5'-AGTTGTCCAGCCCCTTGTAG-3'	anti-sense		
PGP-1 (Mouse)	5'-CTGGATAATTGCCGGTTCTG-3'	sense	60	NM_023217.4
	5'-TCCATGTCGATGATGGAGTC-3'	anti-sense		
GAPDH	5'-TACCCACGGCAAGTTCAACG-3'	sense	60	NM_017008.4
	5'-CACCAGCATCACCCCATTTG-3'	anti-sense		

A.T.: annealing temperature.

5. Characterization spectra

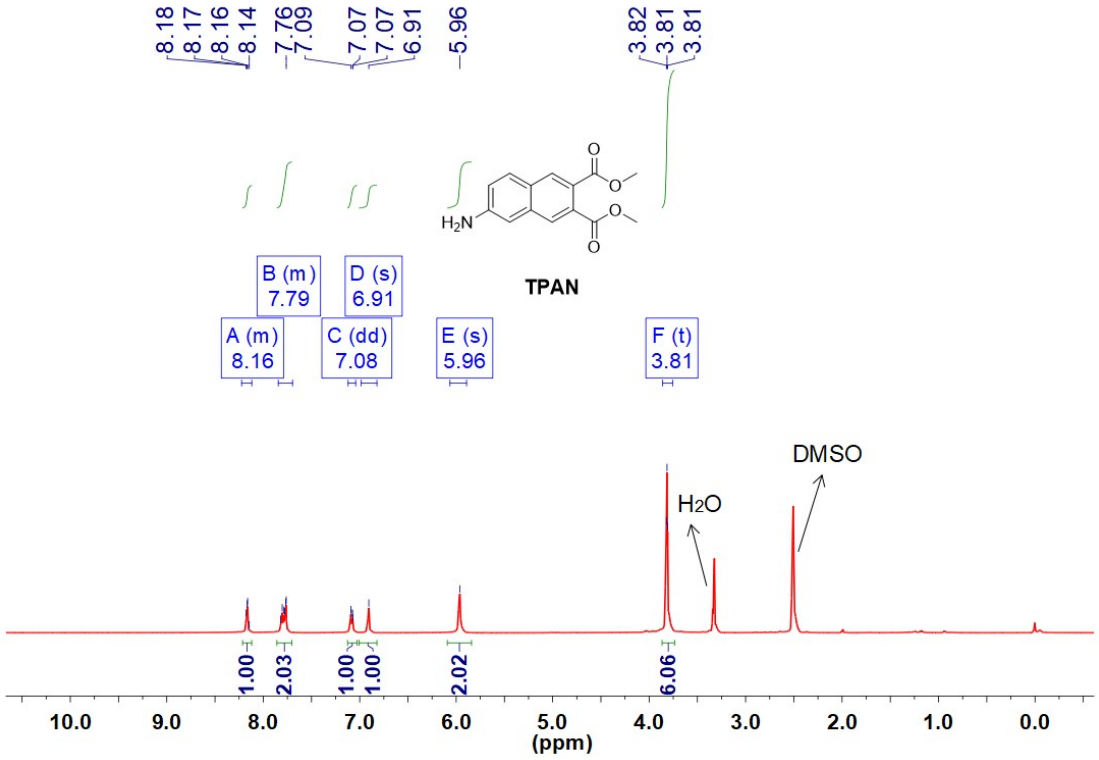

Fig. S13. [1]HNMR spectrum of **TPAN** (500 MHz, 298 K, DMSO-d_6).

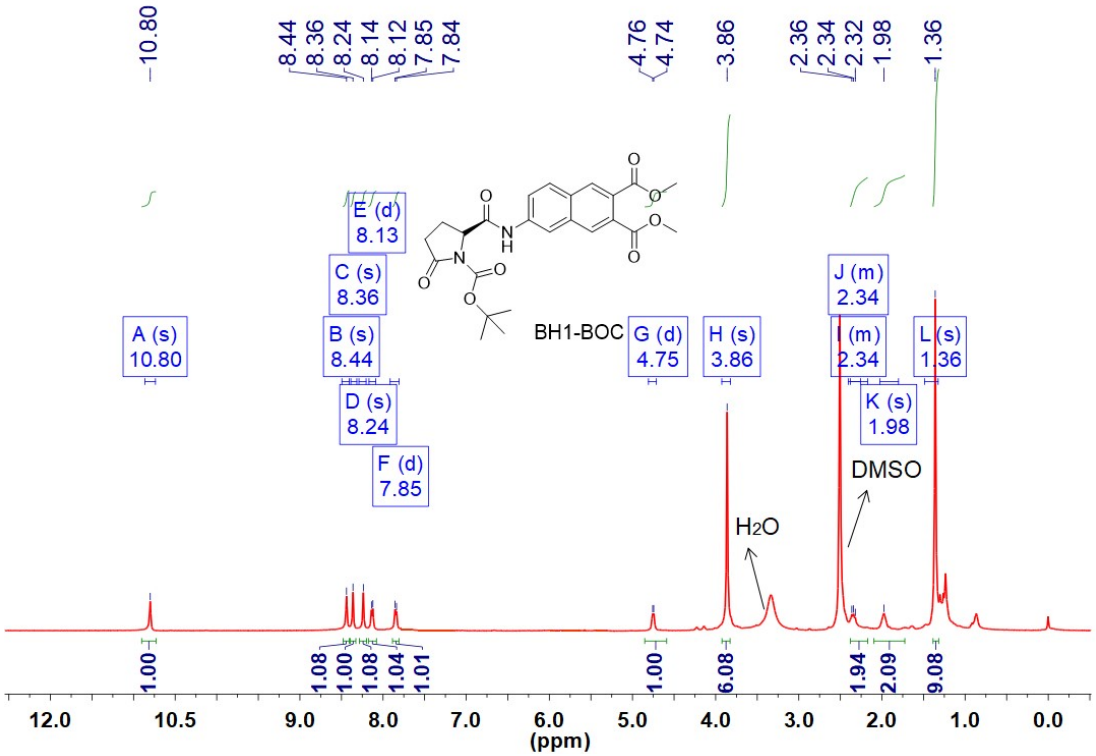

Fig. S14 [1]HNMR spectrum of BH1-BOC (500 MHz, 298 K, DMSO-d_6).

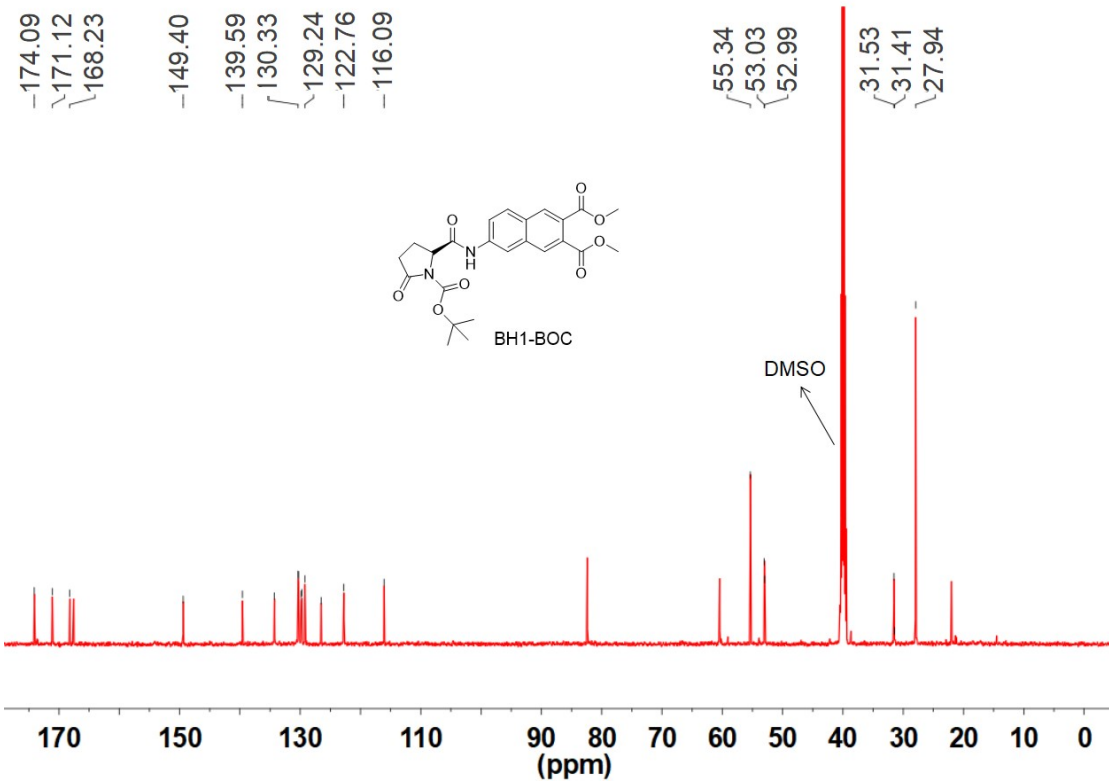

Fig. S15. ^{13}C NMR spectrum of BH1-BOC (125 MHz, 298 K, DMSO-d_6).

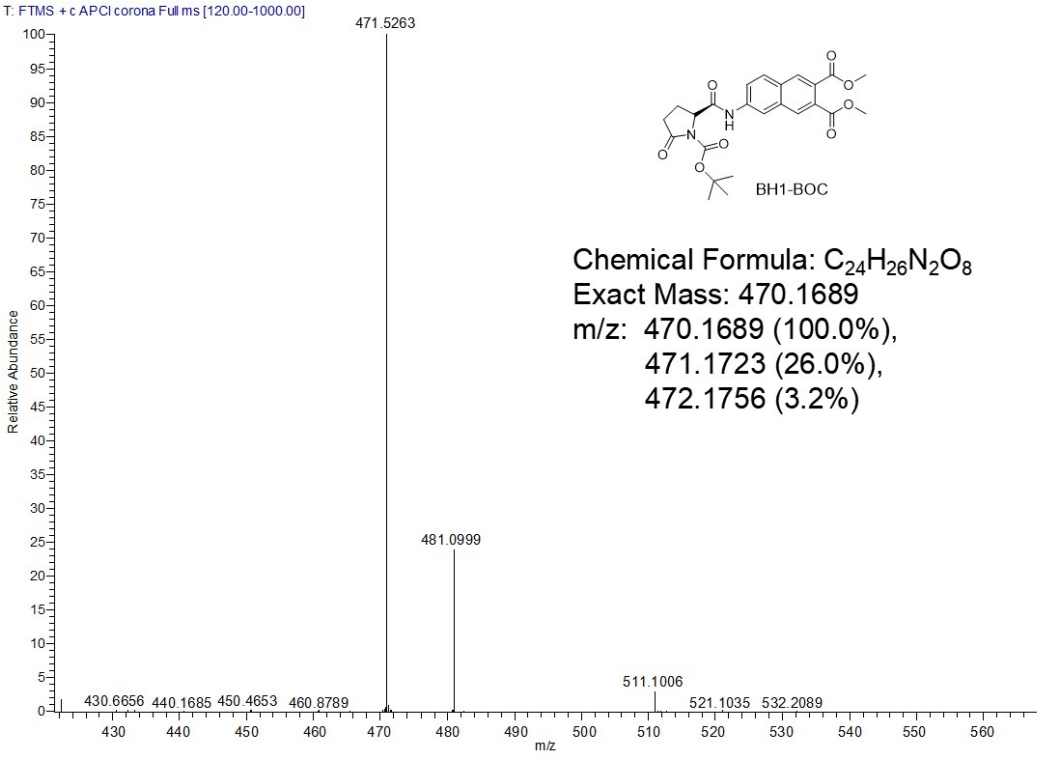

Fig. S16. ESI-MS spectrum of BH1-BOC.

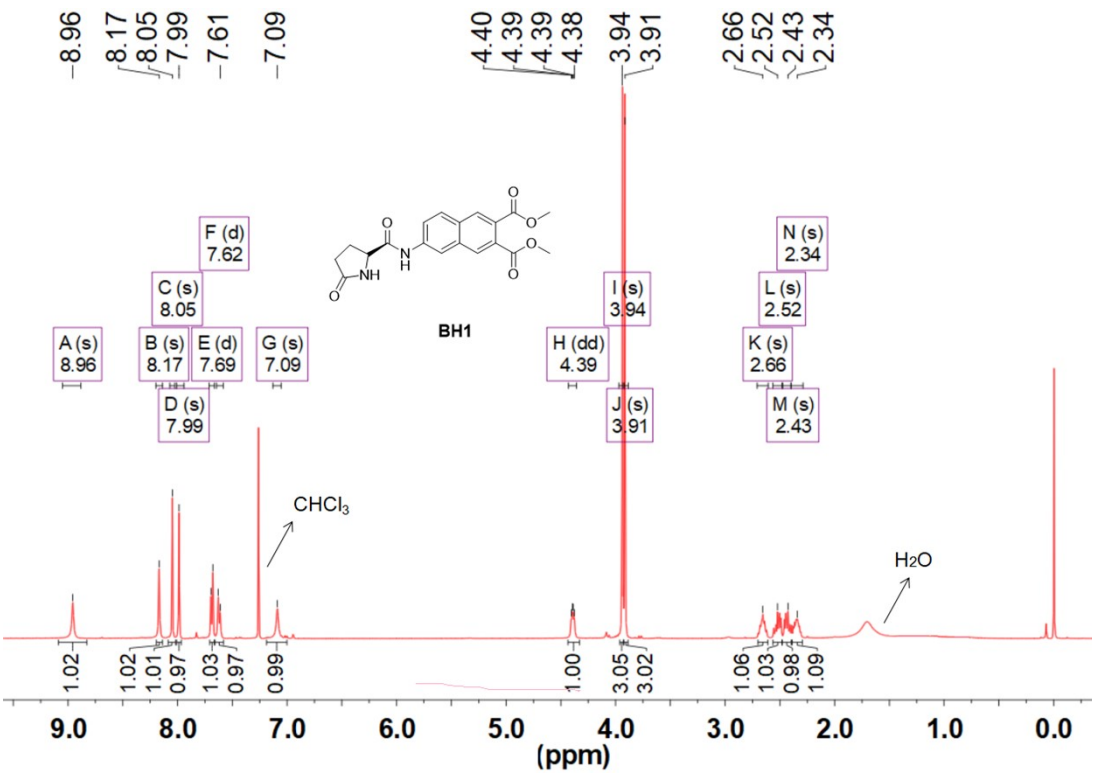

Fig. S17. [1]HNMR spectrum of **BH1** (500 MHz, 298 K, $CDCl_3$).

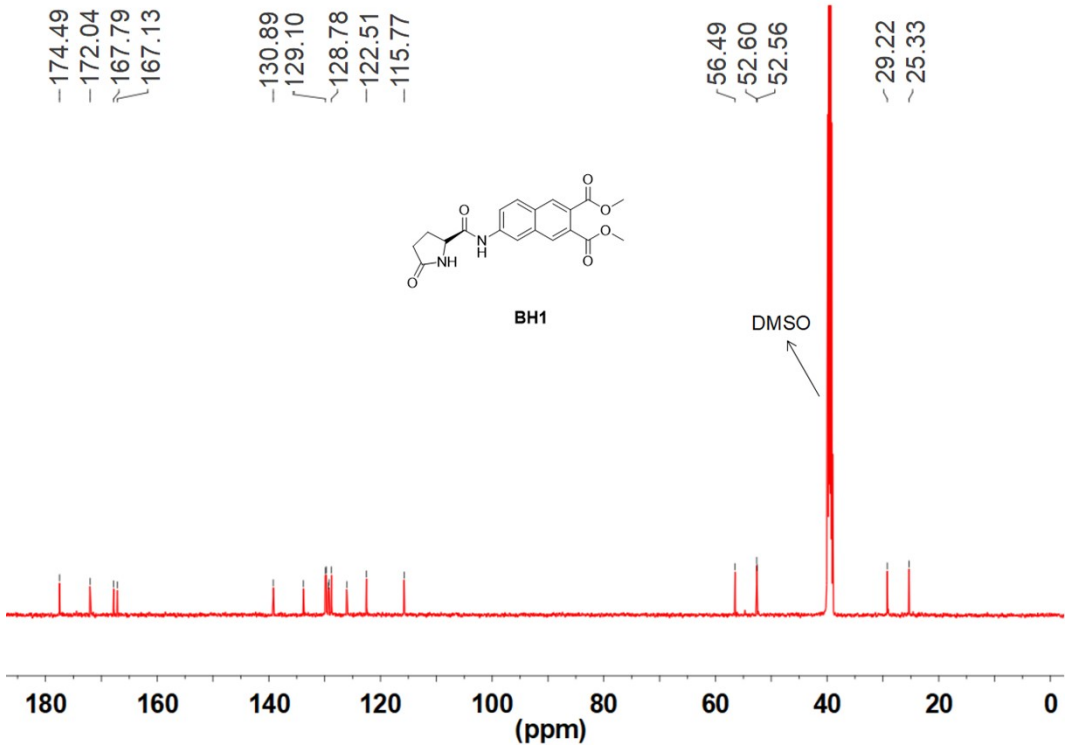

Fig. S18 ^{13}C NMR spectrum of **BH1** (125 MHz, 298 K, DMSO-d_6).

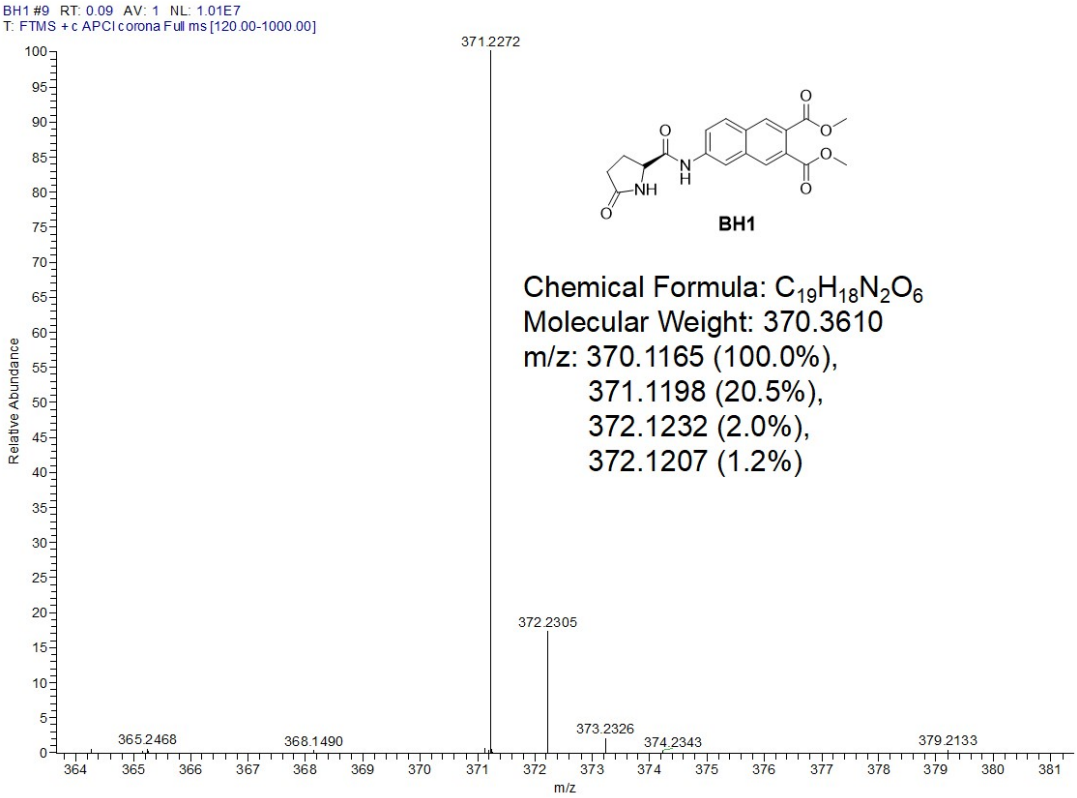

Fig.S19 ESI-MS spectrum of **BH1**.

6. References.

[1] K. Baathulaa, Y. F. Xu, X. H. Qian, *J. Photoch. Photobio. A,* 2010, **216**, 24-34.

[2] T. G. Gray, C. M. Rudzinski, E. E. Meyer, R. H. Holm, D. G. Nocera. *J. Am. Chem. Soc.,* 2003, **125**, 4755-4770.

[3] L. Li, H. Sun, Biochemistry, 2020, 59, 216-217.

[4] M. Z. Zhang, R. N. Su, Q. Zhang, L. Hu, X. H. Tian, Y. Chen, Y. Tian, Sens. Actuators B Chem., 2018, 261, 161-168.